TASK 10 REPORT

PASSIVE FORCE-DEFLECTION TESTS FOR SKEWED ABUTMENTS ON GRAVEL

Prepared By

Kyle M. Rollins, Professor, Civil & Env. Engrg Dept., Brigham Young Univ., 368 CB, Provo, UT 84602, (801) 422-6334, rollinsk@byu.edu

Ian Oxborrow, Research Asst., Civil & Env. Engrg Dept., Brigham Young Univ., 368 CB, Provo, UT 84602, i.oxborrow@gmail.com

Kyle Smith, Research Asst., Civil & Env. Engrg Dept., Brigham Young Univ., 368 CB, Provo, UT 84602, kyle.smith@byu.net

Amy Fredrickson, Research Asst., Civil & Env. Engrg Dept., Brigham Young Univ., 368 CB, Provo, UT 84602, af711.byu@gmail.com

Arthur Guo, Research Asst., Civil & Env. Engrg Dept., Brigham Young Univ., 368 CB, Provo, UT 84602, gzifan@gmail.com

Prepared for

Research Division of the Utah Department of Transportation

September 26, 2014

EXECUTIVE SUMMARY

Accounting for seismic forces and thermal expansion in bridge design requires an accurate passive force-deflection relationship for the abutment wall. Current design codes make no allowance for skew effects on passive force; however, quarter scale lab tests indicate that there is a significant reduction in peak passive force as skew angle increases for plane-strain cases. Further, large scale tests in sand confirmed the findings of the quarter scale tests. To further explore this issue large scale field tests were conducted with skew angles of 0° and 30° in sandy gravel with transverse wingwalls. The abutment backwall was 11 ft (3.35-m) wide by 5.5 ft (1.68-m) high and backfill material consisted of dense compacted sandy gravel. The peak passive force for the 30° skew test was found to be between 61% and 58% of the peak passive force for the 0° skew case. This result is in reasonable agreement with the available laboratory and numerical results; however, discrepancies suggest that the increased stiffness and strength of the gravel backfill has some effect on the reduction in peak passive force with respect to skew angle. Longitudinal displacement of the backwall at the peak passive force was between 3% and 4.5% of the backwall height for the 0° skew test which is consistent with previously reported values for large-scale passive force-deflection tests, but the 30° skew test did not reach a peak even after displacement equal to 7% of the backwall height. Shear force on the backwall increased as skew angle increased despite the reduction in longitudinal force with skew angle. Transverse pile cap displacement also increased with skew angle and was sufficient to mobilize the frictional resistance. Heave geometries for the 0° and 30° tests were quite typically 3% to 4% of the fill height. In all cases the backfill failure geometry extended approximately 4 ft to 5 ft (1.22 m to 1.52 m) beyond the edge of the pile cap and 16 ft (4.88 m) from the face of the cap when measured perpendicular to the backwall.

INTRODUCTION

Numerous large-scale experiments have been conducted with the intent to determine the passive force-deflection curves that might be expected for dense compacted fill behind non-skewed bridge abutments (Mokwa and Duncan 2001; Rollins and Cole 2006; Rollins et al. 2010; Rollins and Sparks 2002). Much of this research indicates that the peak passive force can be accurately predicted using the log-spiral method and is achieved at a longitudinal deflection of 3% to 5% of the backwall height (Rollins and Cole 2006). Methods approximating the complete passive force-deflection curve with a hyperbola have been developed by Shamsabadi et al. (2007) and Duncan and Mokwa (2001). However, for simplicity in design, most specifications recommend a bilinear relationship (AASHTO 2011; Caltrans 2001).

Until recently, no large-scale experiments had been conducted to determine the passive force-deflection relationships for skewed bridge abutments. Furthermore, current bridge design practices assume the peak passive force is the same for skewed bridges as for non-skewed bridges (AASHTO 2011). However, field evidence clearly indicates poorer performance of skewed abutments during seismic events (Apirakyorapinit et al. 2012; Elnashai et al. 2010; Shamsabadi et al. 2006; Unjohn 2012) and distress to skewed abutments due to thermal expansion (Steinberg and Sargand 2010). Laboratory tests performed by Rollins and Jessee (2012) and numerical analyses performed by Shamsabadi et al. (2006) both found that there is a significant reduction in passive force as skew angle increases. Using data obtained from these studies, Rollins and Jessee (2012) proposed the correction factor, R_{skew}, given by Equation (1) which defines the ratio between the peak passive force for a skewed abutment (P_{P-skew}) and the peak passive force for a non-skewed abutment ($P_{P-no\ skew}$) as a function of skew angle, θ.

$$R_{skew} = P_{P-\ skew}/P_{P-no\ skew} = 8.0 * 10^{-5}\theta^2 - 0.018\theta + 1.0 \qquad (1)$$

To more fully understand the relationship between skew angle and reduction in peak passive force, two large-scale tests were conducted to determine the passive force-deflection curves for skew angles of 0° and 30° with sandy gravel backfill. These tests were conducted using an existing 11-ft (3.35-

m) wide by 5.5-ft (1.68-m) high by 15-ft (4.57-m) long pile cap which has been used for a number of previously conducted lateral load and passive force-deflection tests (Rollins et al. 2010; Rollins and Sparks 2002; Strassburg 2010). The 0° skew test for this study was conducted in a similar fashion to the tests conducted by the previous researchers. For the 30° skew test a concrete wedge was attached to the face of the existing pile cap. Testing procedures, results, comparisons to available results, and recommendations based on analysis of the test results are presented in this report.

Previous tests have been performed at these angles at this site with a sand backfill. The two tests in this study used a sandy gravel backfill. Other passive force studies which tested with gravel backfill include Rollins and Cole (2006) and Pruett (2009).

BACKGROUND

As outlined by Burke Jr. (1994) and shown in Figure 1, the interaction of forces at the interface between the bridge abutment backwall and soil backfill may be expressed in terms of the total longitudinal force, P_L, and its components normal to and transverse to the abutment. The normal force is resisted by the passive force, P_P [see Equation (2)]; and the transverse, or shear force, P_T [see Equation (3)], is resisted by the shear resistance, P_R [see Equation (4)]. To prevent instability of the bridge caused by sliding of the abutment against the soil backfill the inequality shown in Equation (5) must be satisfied. In addition, rotation of the entire bridge can occur if the inequality in Equation (6) is not satisfied.
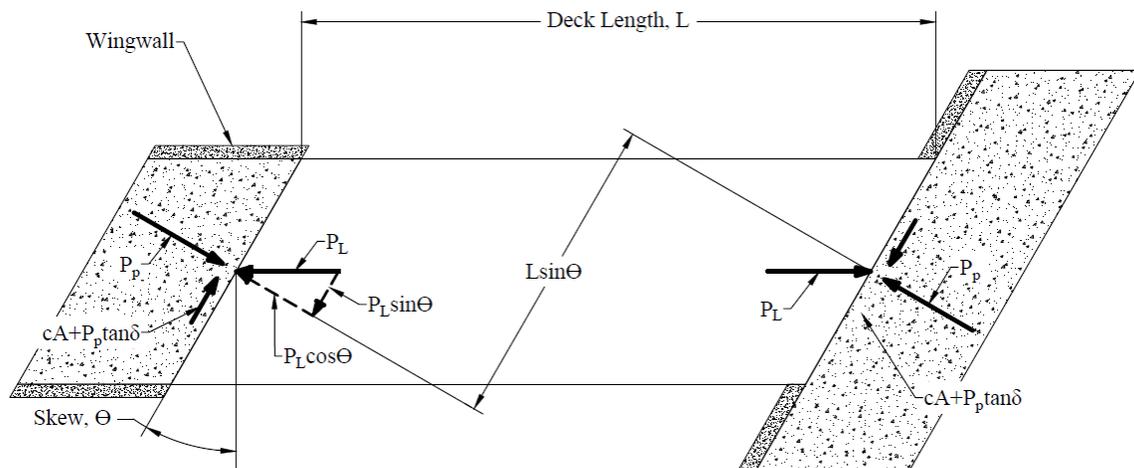
Figure 1. Typical distribution of forces on a bridge with skewed abutments.

$$P_P = P_L \cos\theta \tag{2}$$

$$P_T = P_L \sin\theta \tag{3}$$

$$P_R = cA + P_P \tan\delta \tag{4}$$

$$\frac{cA + P_P \tan\delta}{F_s} \geq P_L \sin\theta \tag{5}$$

$$\frac{(cA + P_P \tan\delta)L \cos\theta}{F_s} \geq P_P L \sin\theta \tag{6}$$

where

$$\theta = \text{skew angle of backwall}$$

$$c = \text{soil cohesion}$$

$$A = \text{backwall area}$$

$$\delta = \text{angle of friction between backfill soil and abutment wall}$$

$$F_s = \text{factor of safety}$$

$$L = \text{length of bridge}$$

These equations are only strictly valid if the bridge remains stable; therefore, if the bridge rotates, the distribution of forces on the abutment backwall will likely change, rendering these equations less accurate. Based on Equation (6), Burke Jr. (1994) noted that if cohesion is ignored the potential for bridge rotation is independent of passive force and bridge length so that at a typical design interface friction angle of 22°, the factor of safety decreases to below 1.5 if bridge skew exceeds 15°.

TEST CONFIGURATION

Test Geometry

The test setup for previous lab tests is shown in Figure 2 and involved a 2 ft (0.61 m) high by 4 ft (1.22 m) wide backwall with a 2D or plane-strain backfill geometry (Rollins and Jessee 2012). In contrast, the field tests used an existing 11 ft (3.35 m) wide by 5.5 ft (1.68 m) high by 15 ft (4.57 m) long pile cap to simulate an abutment backwall as shown in Figure 3. Instead of 2D backfill geometry, the backfill was placed in a test pit that extended a little over 5 ft (1.52 m) out from the sides of the pile cap to

the edge of the test pit with transverse concrete wingwalls to allow for the development of a 3D failure geometry. The backfill extended 24 ft (7.32 m) longitudinally from the face of the pile cap and approximately 1 ft (0.30 m) below the bottom of the cap from the face to 10 ft (3.05 m) from the face to contain the potential failure surface. Though the native soil was significantly stiffer than the backfill materials, the backfill boundaries were considered to be far enough away to not affect the development of a shear surface. Beyond 10 ft (3.05 m), the base of the backfill tapered up to be approximately even with the base of the cap to reduce the required backfill volume.

Load was applied in the longitudinal direction with two 600-kip (2,670 kN) hydraulic actuators which reacted against a sheet pile wall and two 4-ft (1.22 m) diameter drilled shafts that were coupled together by two deep beams.

After conducting the test for the 0° skew conditions, a 30° wedge was attached to the front face of the pile cap for subsequent skew tests as shown in Figure 3. Rollers were placed beneath the wedge to eliminate base friction resistance.
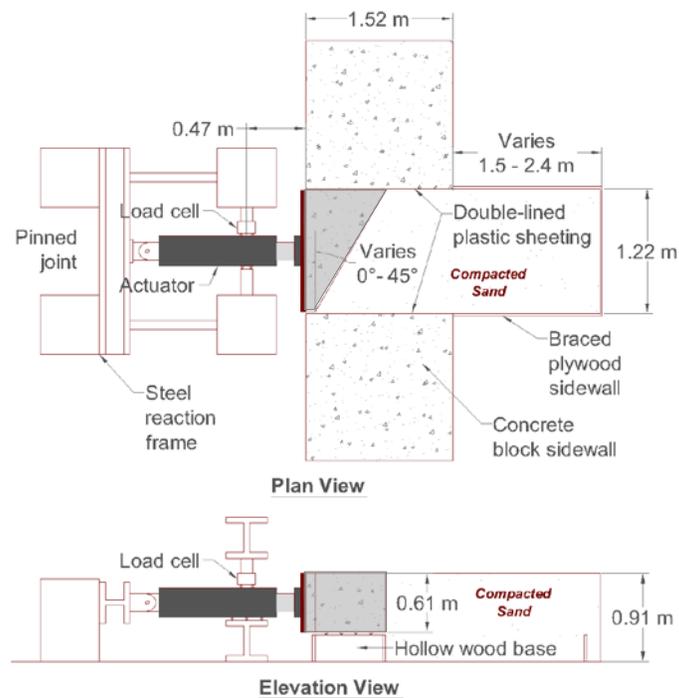
Figure 2. Schematic drawings of lab test layout (Rollins and Jessee 2012) (NOTE 1 m = 3.281 ft).
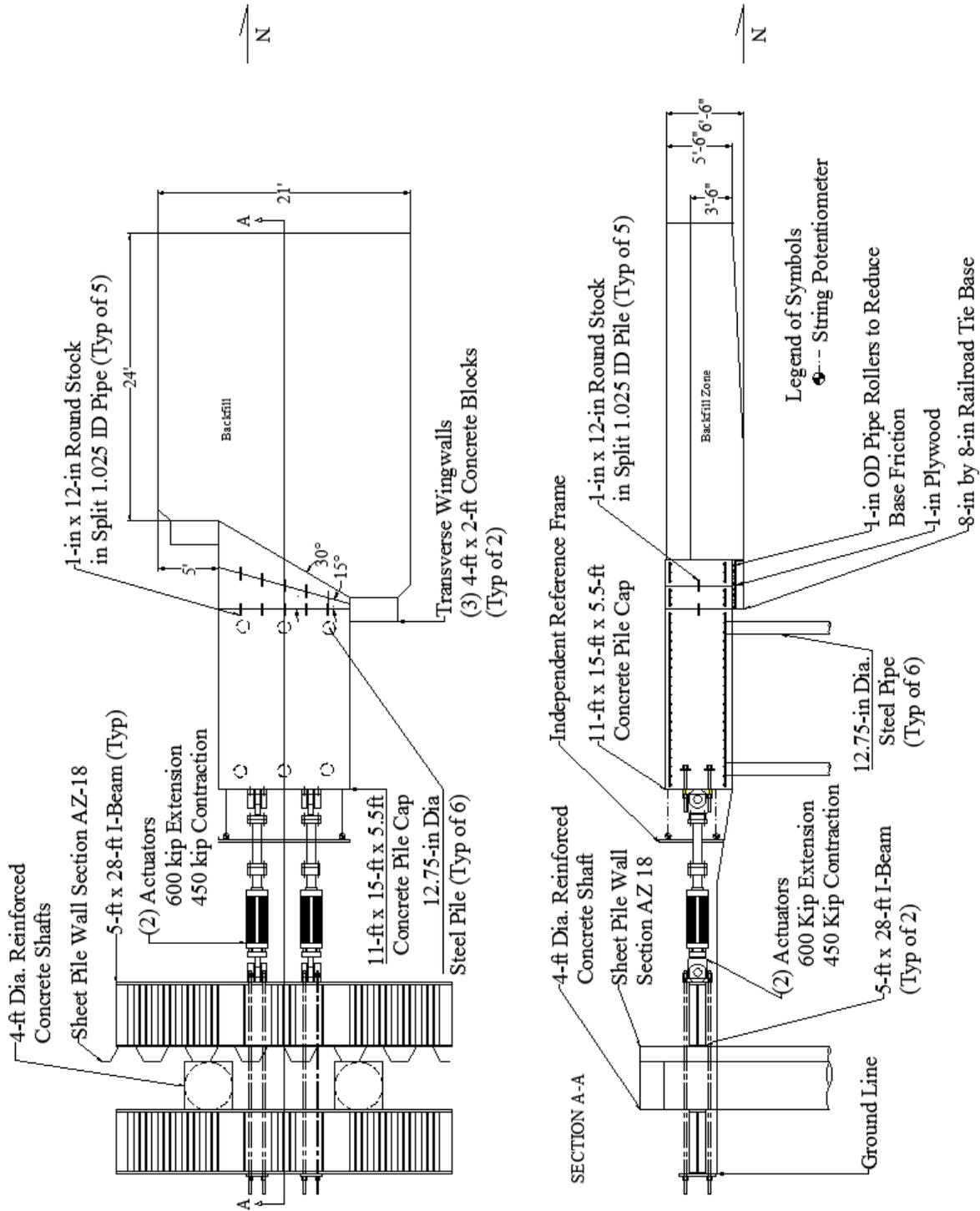
Figure 3. Schematic drawings of field test layout (NOTE 1 ft = 0.305 m).

Instrumentation

   Longitudinal load was measured using pressure transducers in the actuators. Longitudinal displacement of the pile cap was measured using four string potentiometers (string pots) located at each corner of the back of the pile cap and were tied to an independent reference frame. As the piles were assumed to provide vertical restraint, vertical movement of the pile cap was not monitored. Longitudinal and transverse deflection versus displacements data profiles were measured using inclinometers and shape accelerometer arrays (SAAs) which extended approximately 40 ft (14 m) into the center pile in the North and South sides of the pile cap. The shape arrays provided data at 1 ft (0.30 m) intervals while the inclinometers provided data at 2 ft (0.6 m) intervals. Because of the time required to obtain inclinometer readings, the inclinometer measurements were only taken immediately before the start of a test and after the last deflection increment. In contrast, the shape arrays provided profiles at each deflection increment because their collection was instantaneous.

   To measure backfill heave a 2-ft (0.61 m) grid was painted on the backfill surface and the relative elevation of each grid intersection was measured with a survey level prior to, and after conducting each test. Surface cracks in the backfill were also marked following the completion of each test. Figure 4 illustrates the grid and cracks at the end of the 0° skew test. For that particular test, the 6 ft nearest to the pile cap was gridded at 1-ft intervals.

Geotechnical Backfill Properties

   Backfill material consisted of a well-graded gravel with silt and sand (GW-GM or A-1-a as classified by the Unified Soil Classification System and AASHTO classification system, respectively). As shown Figure 5, two gradation tests were performed on the backfill by Staker, the supplier The particle-size distribution generally falls within the gradation bounds specified for the subsequentr Geosynthetic Reinforced Soil (GRS) tests, as shown in Figure 5. It also correlates well to the dense coarse gravel used in Rollins and Cole (2006), though with significantly more gravel and less sand

and fines material than Pruett (2009). The gradations of the backfill performed by the supplier and one

performed at the BYU Soil Mechanics lab are shown.

Figure 4. Non-skewed instrumentation, end of test
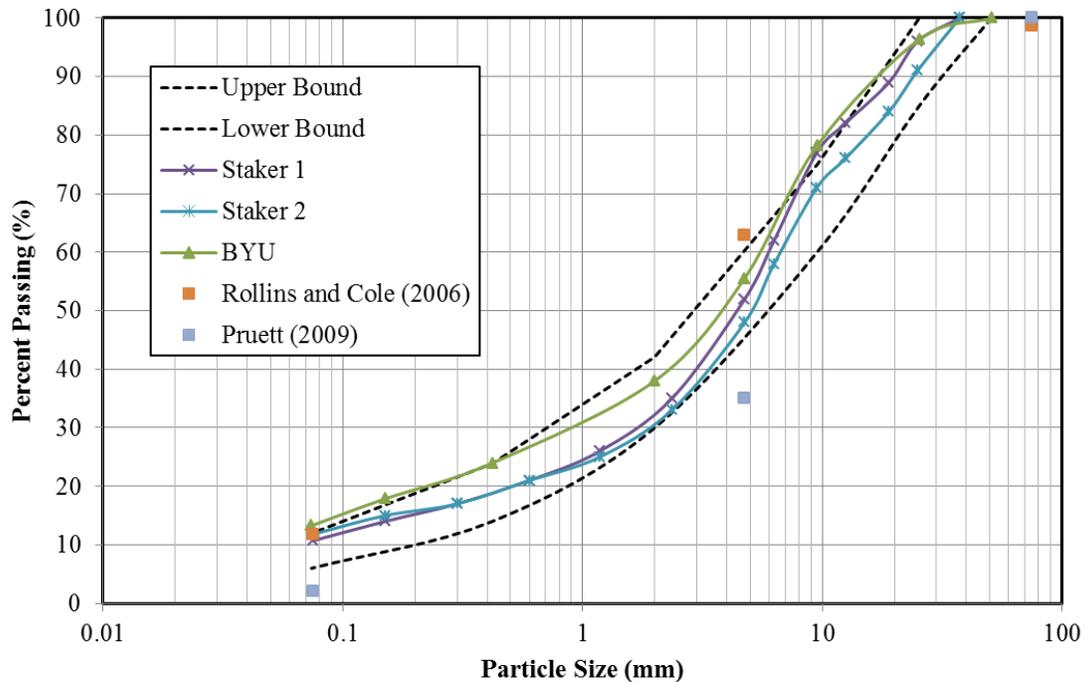
Figure 5. Gradation for backfill gravel relative to specified limits.

Unit Weight and Moisture Content

Maximum dry unit weight according to the modified Proctor compaction test (ASTM D1557) performed prior to testing was 142.0 lb/ft^3 (22.3 kN/m^3) and the optimum moisture content was 6.3%. The target on-site compaction level was 95% of the modified Proctor maximum. Backfill gravel was placed in lifts approximately 4- to 6-in (15.24-cm) thick and compacted with a smooth-drum vibratory roller and a walk-behind vibratory plate compactor to an average density greater than 95% of the modified Proctor maximum. A nuclear density gauge was used to obtain relative compaction and water content data during compaction. Though not shown, the variation of relative compaction and moisture content with depth was not significant. Relative density was estimated using the empirical relationship between relative density (D_r) and relative compaction (R) for granular materials developed by Lee and Singh (1971) as shown in Equation (7), where D_r and R are measured in percent.

$$R = 80 + 0.2D_r \tag{7}$$

A summary of the soil density and water content measurements for the two tests is shown in Table 1. The properties of the two backfills were generally very consistent. Average relative compaction, relative density, and water content for the two tests were 96.3%, 81.5%, 7.1%, respectively. For comparison purposes the average relative compaction, relative density, and water content for the laboratory tests with sand were 97.9%, 90%, and 8.0%, respectively (Rollins and Jessee 2012).

TABLE 1 Summary of Compaction and Water Content Data for Each Test

Backfill Soil Properties	0⁰ Skew Test	30⁰ Skew Test
Minimum Dry Unit Weight [pcf]	133.7	133.7
Maximum Dry Unit Weight [pcf]	141.7	139
Average Dry Unit Weight [pcf]	136.2	137.3
Relative Compaction	95.9%	96.7%
Relative Density	79.5%	83.5%
Moisture Content	6.4%	7.8%
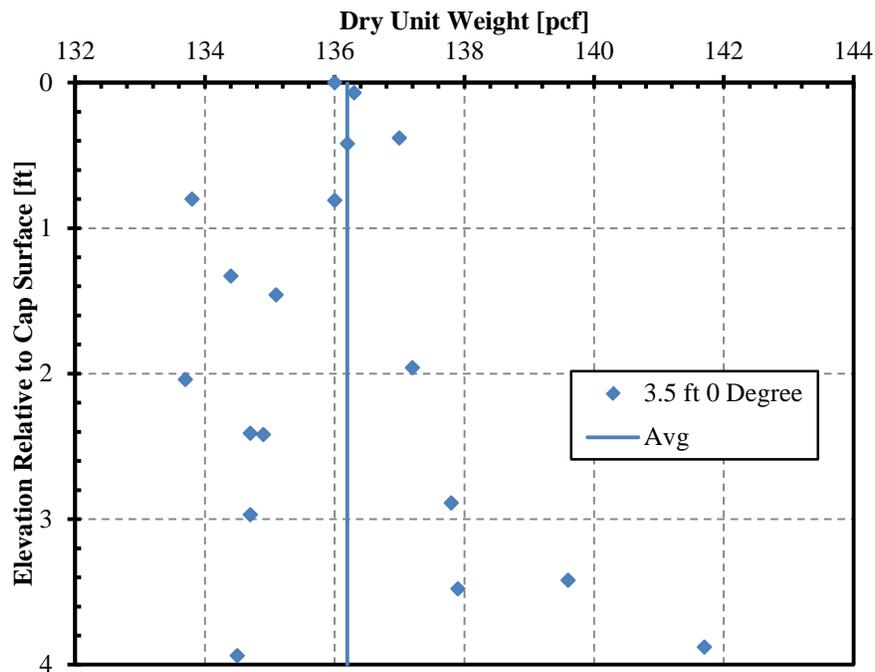
Figure 6. Dry unit weights for 0° skew
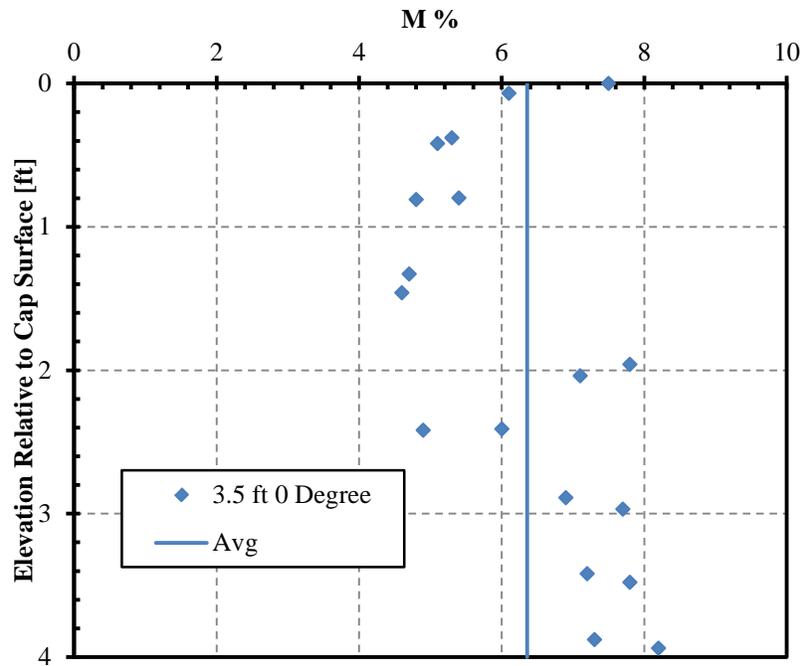
Figure 7. Moisture contents for 0° skew
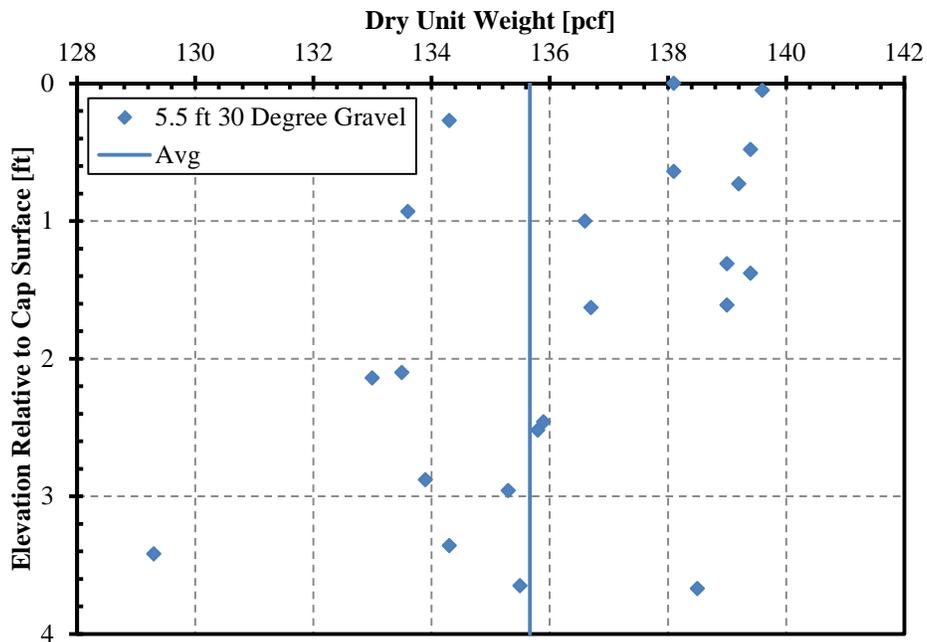
Figure 8. Dry unit weights for 30° skew
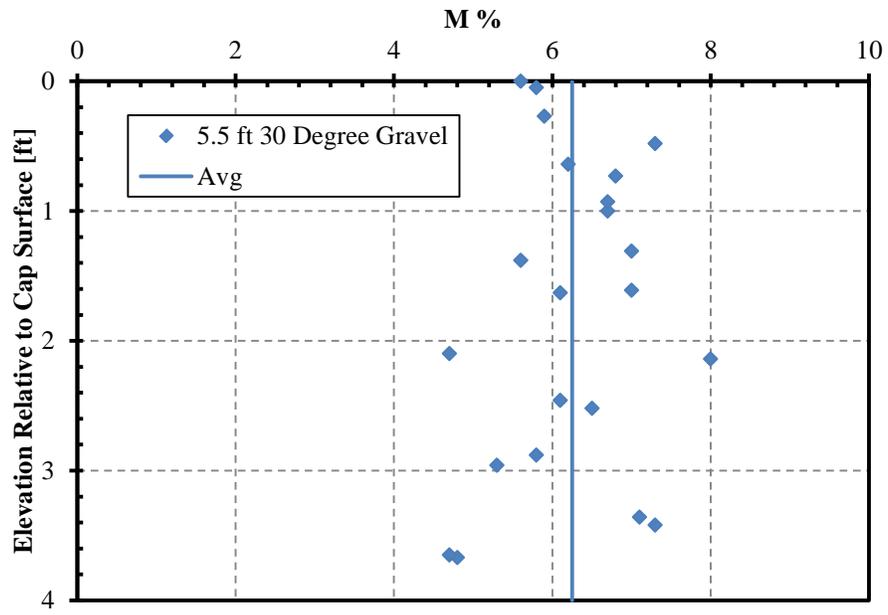
Figure 9. Moisture contents for 30° skew

Shear Strength

In situ direct shear tests were conducted for the gravel backfill. Figure 10 shows how the box shear tests were performed. The tests were performed after the non-skewed 3.5 ft gravel test, so the backfill was at 95.9% compaction. The box was carefully lowered into place by chipping away the soil around the box and tapping the box downward, into the backfill. Once in place, weights were loaded on top of the soil and a hydraulic jack was used to apply the lateral force. Displacement was measured with a dial gauge.

Two independent tests were performed and the results are shown in Figure 11. The drained friction angle (ϕ') was found to be 45.8° with a cohesion of 40 lbs/ft^2 (6.3 kN/m^2) Previous researchers (Rollins and Cole 2006) conducted direct shear tests and determined that the interface friction angle (δ) between similar coarse gravel soil and concrete was about 75% of the soil friction angle.

Figure 10. In situ box direct shear test on gravel backfill
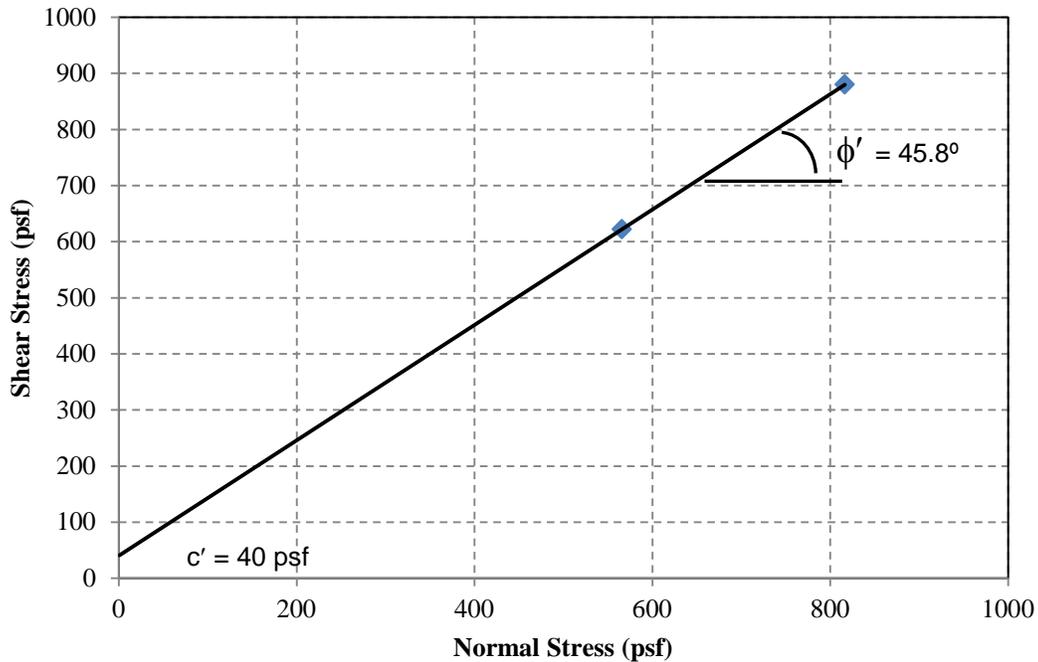
Figure 11. In situ box direct shear results for gravel backfill

General Test Procedures

Prior to testing with the backfill in place, a lateral load test was performed to determine the "baseline" resistance of the pile cap alone, and the pile cap with attached wedge. Because the pile cap had been previously employed for a number of tests, the baseline resistance has become relatively linear. Following the baseline test, backfill was compacted adjacent to the cap and a lateral load test was performed to obtain the total resistance. Following backfill compaction, the surface grid was painted and appropriate initial measurements, including relative elevations of the grid points, were recorded. The backfill material was completely excavated and recompacted for each individual test.

The pile cap (and attached wedge if applicable) was then pushed longitudinally into the backfill zone in 0.25-in (6.35-mm) increments at a velocity of 0.25 in/min (6.35 mm/min) to a final displacement of 3.25 in to 3.75 in (8.30 cm to 9.53 cm) using the two hydraulic actuators. The 5.5 ft 30° test was only pushed to 2.50 in due to the increased resistance of the gravel compared to the sand tests and the limited capacity of the actuators. At each 0.25-in (6.35-mm) displacement increment the load was held for

approximately 2 minutes to observe the reduction in longitudinal force against the backwall as a function of time. On average, the reduction in force after 2 minutes was about 9%.

A plot of the total load and corresponding baseline curve for the non-skewed test is shown in Figure 12. The resistance of the pile cap in the longitudinal direction is made up of the combined passive and shear resistances of the pile cap [see Equations (2) and (3)]. This combined resistance is represented by the difference between the total and baseline curves.

TEST RESULTS

Passive Force-Deflection Curves
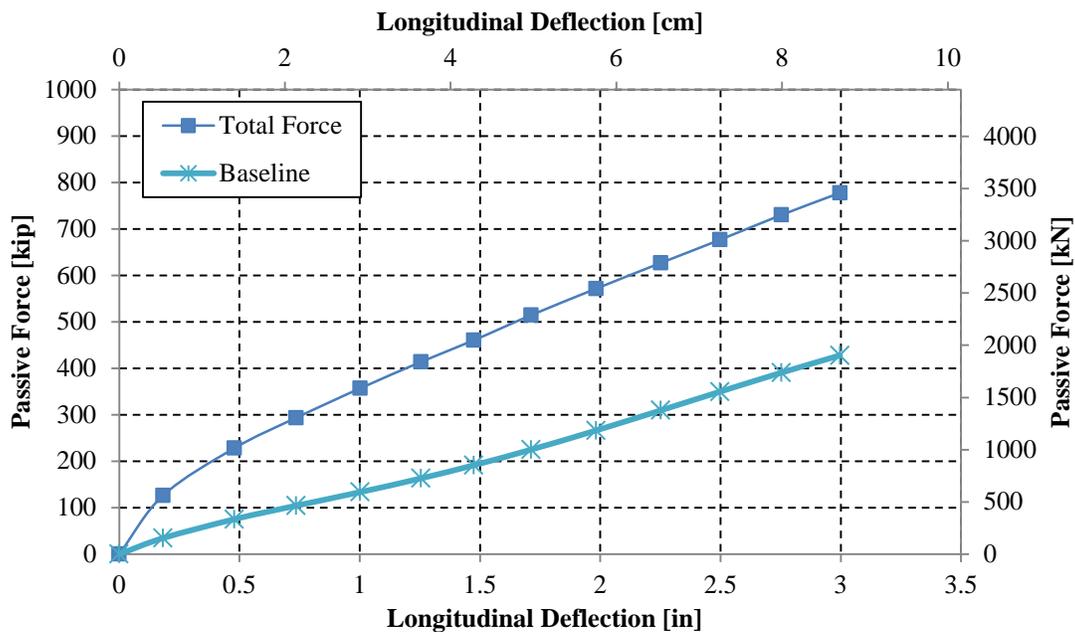
Figure 12. Total force and baseline resistance for 0° skew test.

Figure 12 shows the total force versus longitudinal deflection curves for the non-skewed gravel field test. Passive force was calculated from the total actuator load corrected for the appropriate baseline curve using Equation (2). Backwall deflection was computed as the average deflection of the four string pots on the back of the pile cap. The 30° test passive force was calculated in similar manner, as discussed below.

After performing the 30° skew test using a gravel backfill height of 5.5 ft, as was previously done in testing with sand backfill, the resulting data suggested that the 0° skew test to be performed with gravel backfill would likely exceed the 1200 kip load capacity of the two actuators. Therefore, for the 0° skew test the gravel backfill was only compacted to a height of 3.5 ft. To allow comparisons between the two tests, the load from the 30° test with the 5.5-ft thick backfill was scaled down to a 3.5-ft thickness by the square of the ratio of the heights, H, based on Equation (8) below:

$$P_P = \frac{1}{2}\gamma H^2 K_P B_e + 2cHB_e\sqrt{K_P} \qquad (8)$$

where the parameters γ, K_P, and B_e are dry unit weight, passive lateral earth pressure coefficient, and the effective width, respectively, but are irrelevant to the scaling of the passive force, P_P. Cohesion, c, is assumed to be small, leaving only the first term to be evaluated. Therefore, the 30° skew 5.5 ft passive force values were multiplied by the scale factor $(3.5 \text{ ft})^2 / (5.5 \text{ ft})^2$, or 0.40, to obtain the scaled 3.5 ft passive force values for the 30° test. While this represents a first approximation of the likely results, additional corrections to account for geometrical differences and cohesion will be explored before the final report.
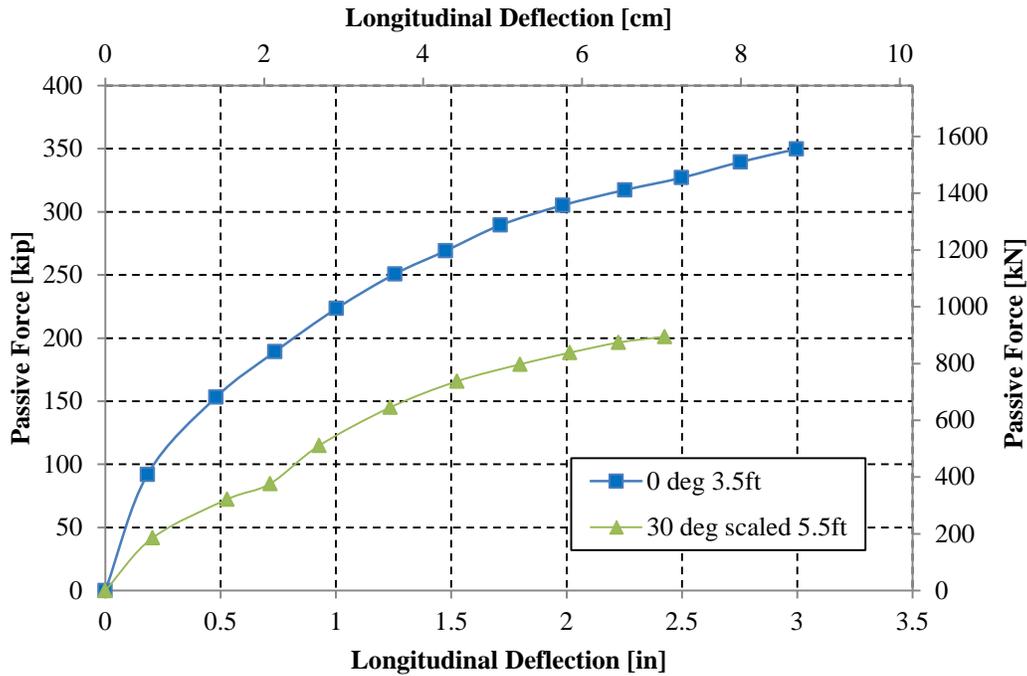
Figure 13. Comparison of passive force versus longitudinal deflection for 0° and 30° skew

Figure 13 shows passive force versus longitudinal deflection curves for both tests. For the 30°

skew test it appears that the resistance was nearing the peak resistance at the end of the test which

represents a displacement equal to about 3.75% of the 5.5 ft wall height. Because of the skew angle, the

force on the west actuator reached capacity and the test could not be continued to greater displacements.

For the 0° skew test, the peak was not reached, although the cap displacement was already at 7% of the

wall height. The testing system, however, does not allow for displacements much larger than 3.5 inches,

and the baseline curve greater than 3.0 inches in some cases appears questionable, perhaps due to the high

volume of tests performed with this testing system and pile cap.

Figure 14 plots the passive force reduction factor versus skew angle for the lab tests conducted by

Rollins and Jessee (2012), the numerical models reported by Shamsabadi et al. (2006), and the results of

this study with a gravel backfill. As can be seen from Figure 14, Equation (1) predicts that at the skew

angle 30° the passive force reduction factor should be 50% when compared to the 0° skew case in gravel.

If the peak values for the 0° and 30° skew tests are used as has been done in previous tests a a reduction factor of 58% is obtained when comparing the 30° skew test to the 0° skew test. However, if the resistance values are compared at a displacement of 2.5 in, the reduction factor is 0.62. These results suggest that the force reduction factor equation is generally applicable for gravel but may require some fine tuning because of the increased stiffness and friction angle of gravel backfill compared to sand backfill.
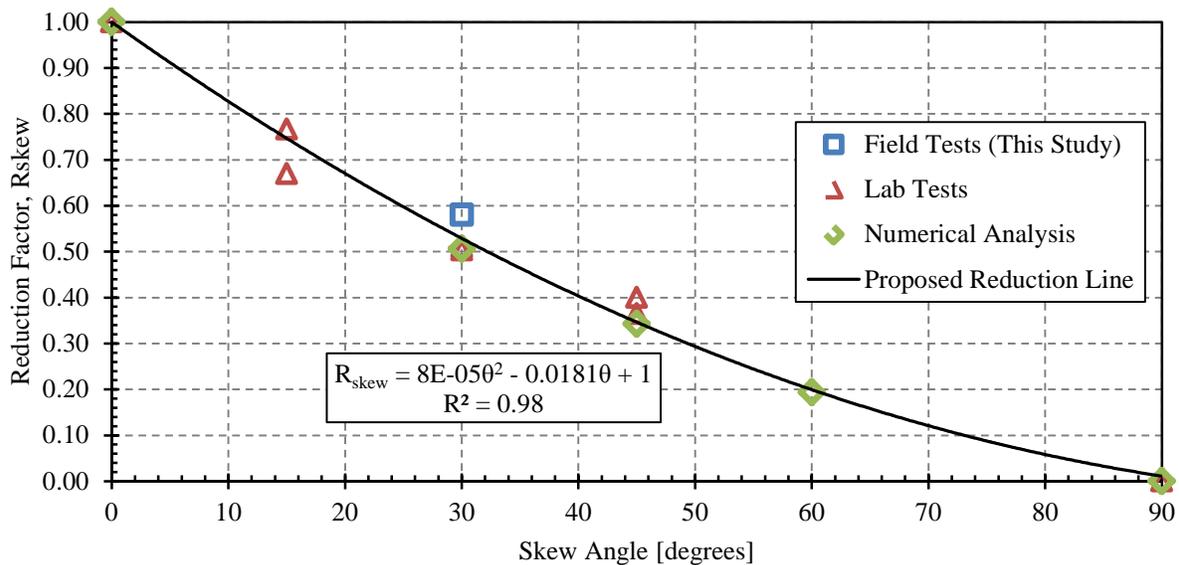
Figure 14. Reduction factor, R_{skew} (passive force for a given skew angle normalized by passive force with no skew) plotted versus skew angle based on lab tests (Rollins and Jessee 2012), numerical analyses (Shamsabadi et al. 2006) and results from field tests in this study.

Pile Cap Displacement vs. Depth

Figure 15 provides longitudinal deflection versus depth profiles obtained from both an inclinometer and a shape accelerometer array for the 0° skew test. A similar profile is shown in Figure 16 but excludes the inclinometer reading since a reliable post-test inclinometer reading was not obtained for the 30° test. Both profiles represent pile cap behavior for the final longitudinal displacement of the test. The depths are referenced to the top of the cap. The average deflection measured by the string pots at two elevations on the pile cap are also shown in Figure 15 and Figure 16 for comparison purposes. Figure 15 demonstrates that the measurements for the three systems are reasonably accurate and aligned with each

other. The percent difference between the inclinometer and shape array profiles for the non-skewed test from the top of the cap to a depth of 16 ft (4.9 m) ranges between 0.03% and 13% with an average of about 6%. The displacements below a depth of 16 ft (4.9 m) are small and the error values in this zone are not particularly meaningful.
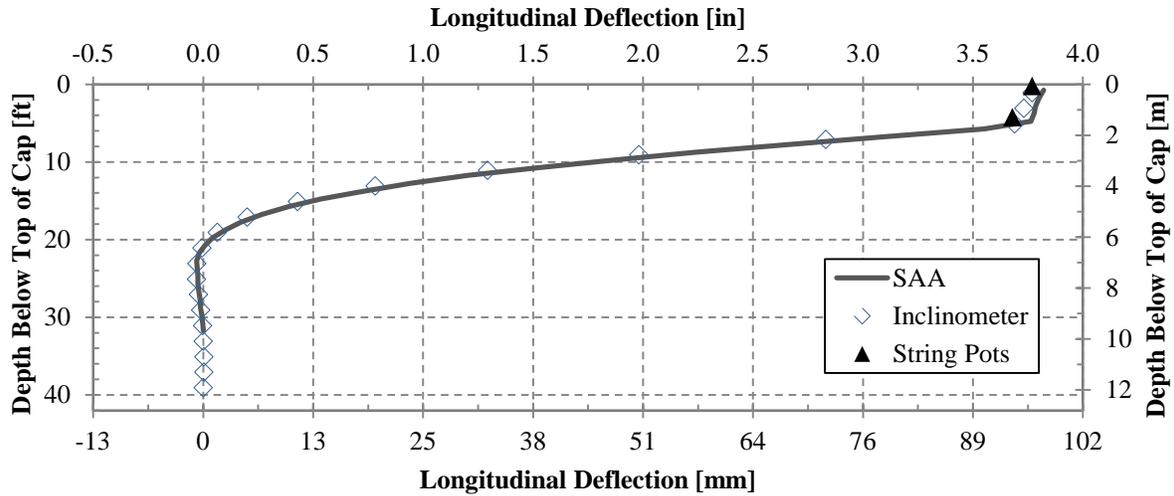
Figure 15. North 3.5-ft backfill 0° skew final deflection comparing inclinometer, shape array, and string potentiometers.
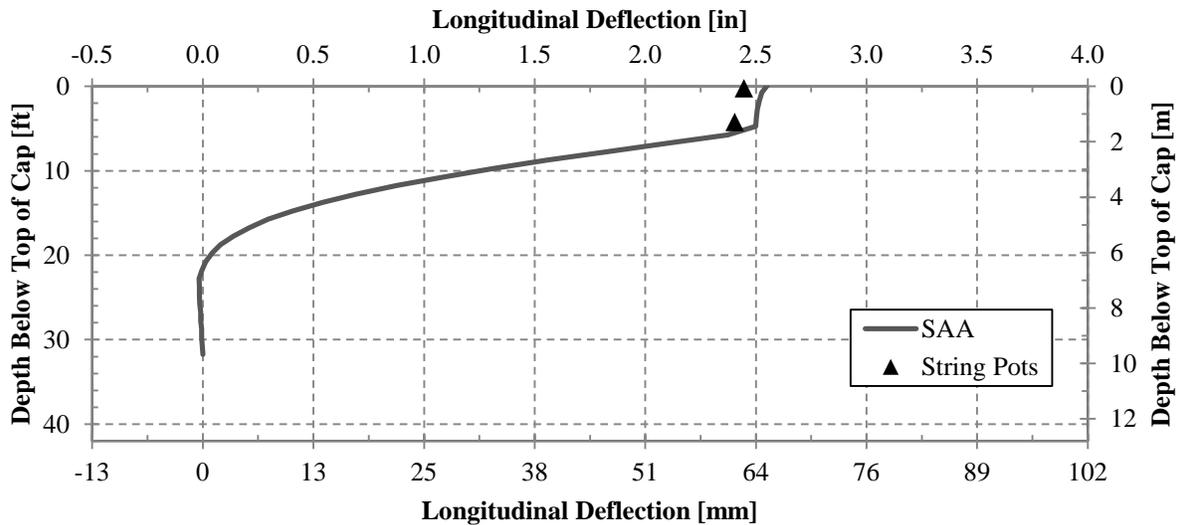
Figure 16. North 5.5-ft backfill 30° skew final deflection comparing shape array and string potentiometers

The measurements indicate a relatively linear deflection profile within the pile cap and small cap rotations. Below the base of the cap, the piles deflect in a non-linear fashion with the deflections reaching a point of counterflexure at depth of approximately 22 ft (6.7 m) and a point of fixity at about 30 ft (9.1 m). Agreement between the north and south inclinometers was generally very good.

Transverse deflection versus depth profiles for the pile cap, recorded by shape array and inclinometer, are plotted in Figure 17 and Figure 18. Plotted on a smaller scale, the percent error seems larger than the longitudinal error though the magnitude difference is very small. However, as observed for the deflections below 16 ft (4.9 m) in the longitudinal test, the percent difference is exaggerated due to the smaller scale. The percent difference is within the error thresholds of each instrument (±1.5 mm/30 m for shape array and ±1.24 mm/30m for inclinometer) (Rollins et al. 2009). Once again, the shape of the deflection profile indicates essentially linear deflection in the pile cap and very small rotations. The deflection in the piles is non-linear and decreases to zero at a deflection of about 30 ft (9.1 m).
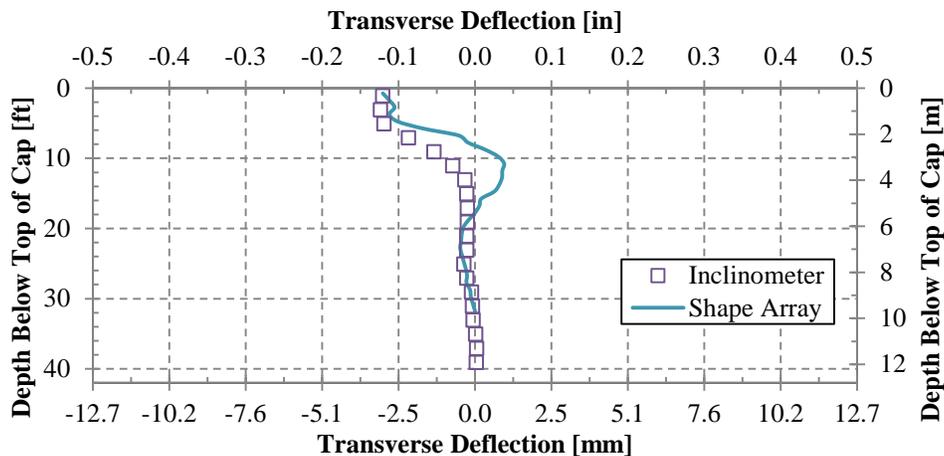
Figure 17. North 3.5-ft backfill 0° skew final deflections comparing inclinometer and shape array

Transverse Deflection [in]

Depth Below Top of Cap [ft]

Depth Below Top of Cap [m]

Transverse Deflection [mm]
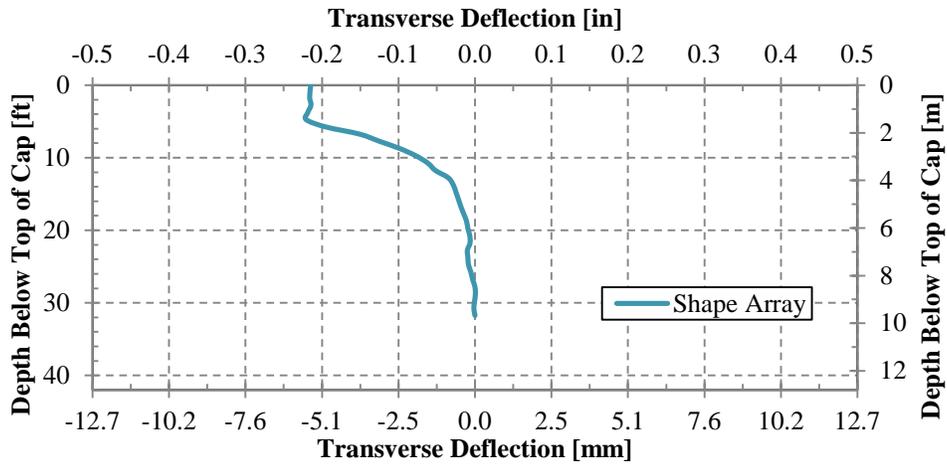
Figure 18. North 5.5-ft backfill 30° skew final deflections according to shape array measurements

Longitudinal Deflection [in]

Depth Below Top of Cap [ft]

Depth Below Top of Cap [m]

Longitudinal Deflection [mm]
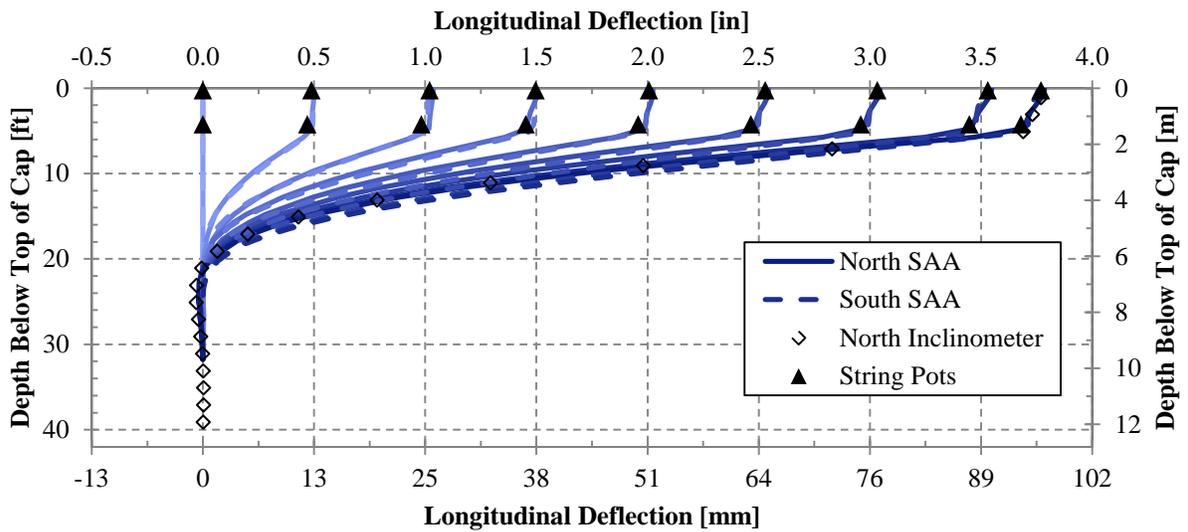
Figure 19. Longitudinal deflection vs. depth curves for 0° skew 3.5 ft test from string potentiometer and SAA data at various deflection increments and the final north inclinometer reading
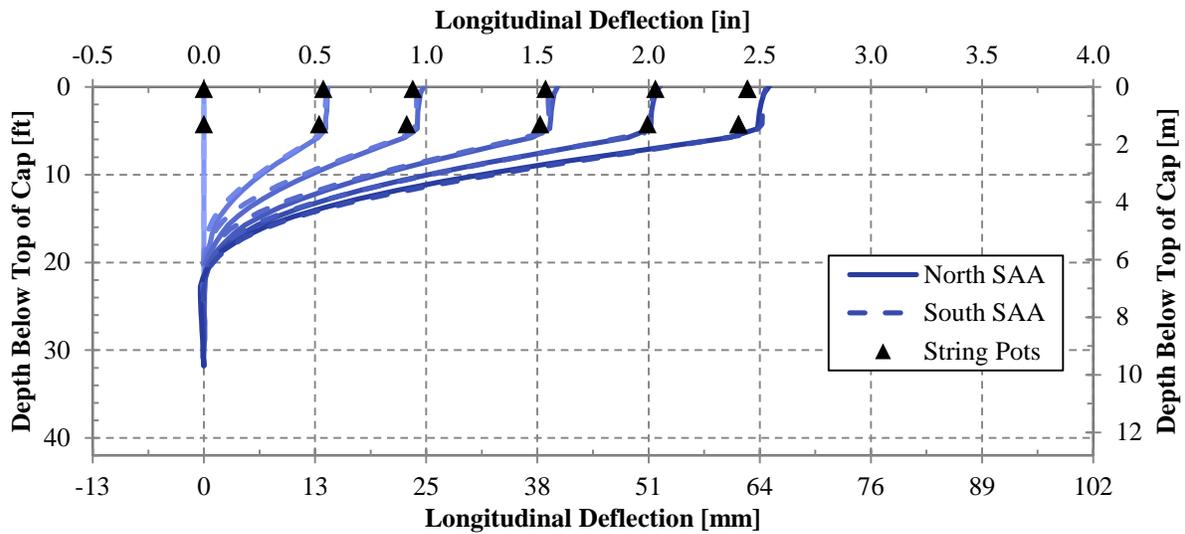
Figure 20. Longitudinal deflection vs. depth curves for 30° skew 5.5 ft test from string potentiometer and SAA data at various deflection increments

Although the inclinometer readings were only taken at the maximum deflection for each load test, shape array profiles in the longitudinal and transverse directions were obtained at each deflection increment for each test. Figure 19 shows profiles of longitudinal deflection vs. depth for each deflection increment. As the deflection level increases the deflection of the pile cap remains linear, the rotation progressively increases, and the depth to the point of fixity increases. Similar curves were obtained in the transverse direction. At smaller deflection levels there are some variations associated with the small measurement errors; however at larger deflections, the data was accurate and useful in visualizing the pile movement. The small variation in the 30° scaled test (Figure 20) between the shape array and string pot data at some increments is likely an effect from missing the inclinometer reading from this test as previously discussed. An inclinometer reading is necessary to calibrate the rotational orientation of the shape array data most accurately.

The measured transverse deflections at the top of pile cap, as measured by inclinometer and shape arrays, on both the north and south sides of the cap after the last deflection increment for each test are plotted in Figure 21 from a plan view perspective. By connecting these points on the north and south

sides, the rotation of the cap can be visualized. Although deflections of both actuators were kept relatively constant throughout the test, rotation and transverse deflection were still affected by the skew angle. As seen in Figure 21, for both the 0° and 30° skews the pile cap ultimately shifted to the left (the direction of the 30° skew) by approximately 0.09 and 0.15 inch, respectively, and rotated in a counterclockwise direction approximately 0.02° and 0.05°, respectively. The transverse movement of the 0° test may be attributed to the number of skewed tests performed on the piles that have weakened the resistance to pile movement to the west as the cap is pushed north.
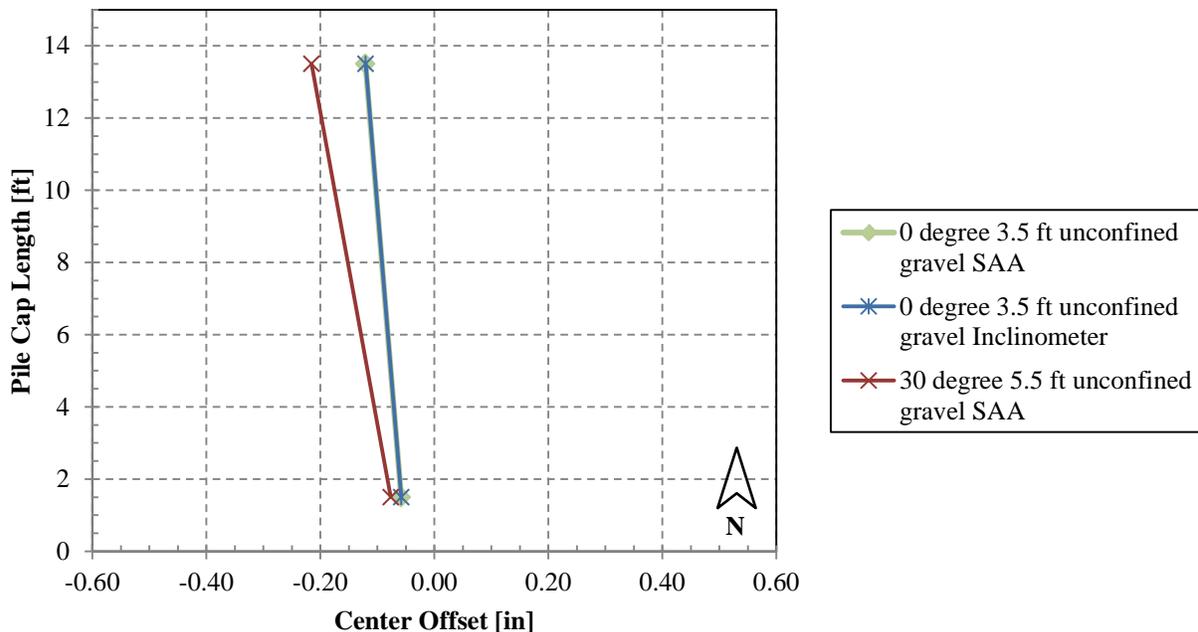
Figure 21. Transverse pile cap deflection and rotation determined between north and south shape array and inclinometer data

Applied Shear Force vs. Transverse Displacement

The relationship between the applied shear force (P_T) and transverse displacement is plotted in Figure 22 for the 30° skew test. The applied shear force was computed using Equation (3) and displacement values were based on shape array measurements taken during testing. The unusual decrease in transverse displacement is due to the cyclic loading performed at the 0.5 inch longitudinal displacement (0.08 in transverse displacement). When this test resumed to the 0.75 inch longitudinal displacement,

transverse displacement had shifted some to the positive direction, the east. The data shows a consistent

shear force-displacement curve despite the shift from the cyclic loading. The shear force appeared to be

approaching a peak when the testing finished, similar to the passive force for this test. The curve did not

seem to agree with previously performed tests on the 30° skew in sand, but a comparison between this test

and the GRS 30° skew test will be included into the Task 11 report.
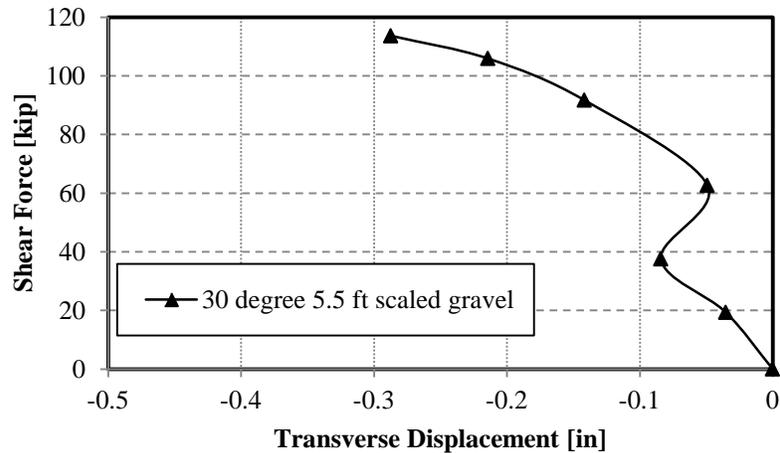
Figure 22. Applied shear force versus transverse displacement

Failure Surface Geometry

Backfill heave contours and surface cracks for the non-skewed and 30° skewed abutments are

illustrated in Figure 23 and Figure 24. Surface cracks for this test were also pictured earlier in Figure 4.

Heave contours for the non-skewed abutment are generally symmetrical with maximum heave (4.4 in)

occurring 2 ft from the backwall near the abutment edges. Surface cracks develop as far as 14 ft out from

the non-skewed backwall.
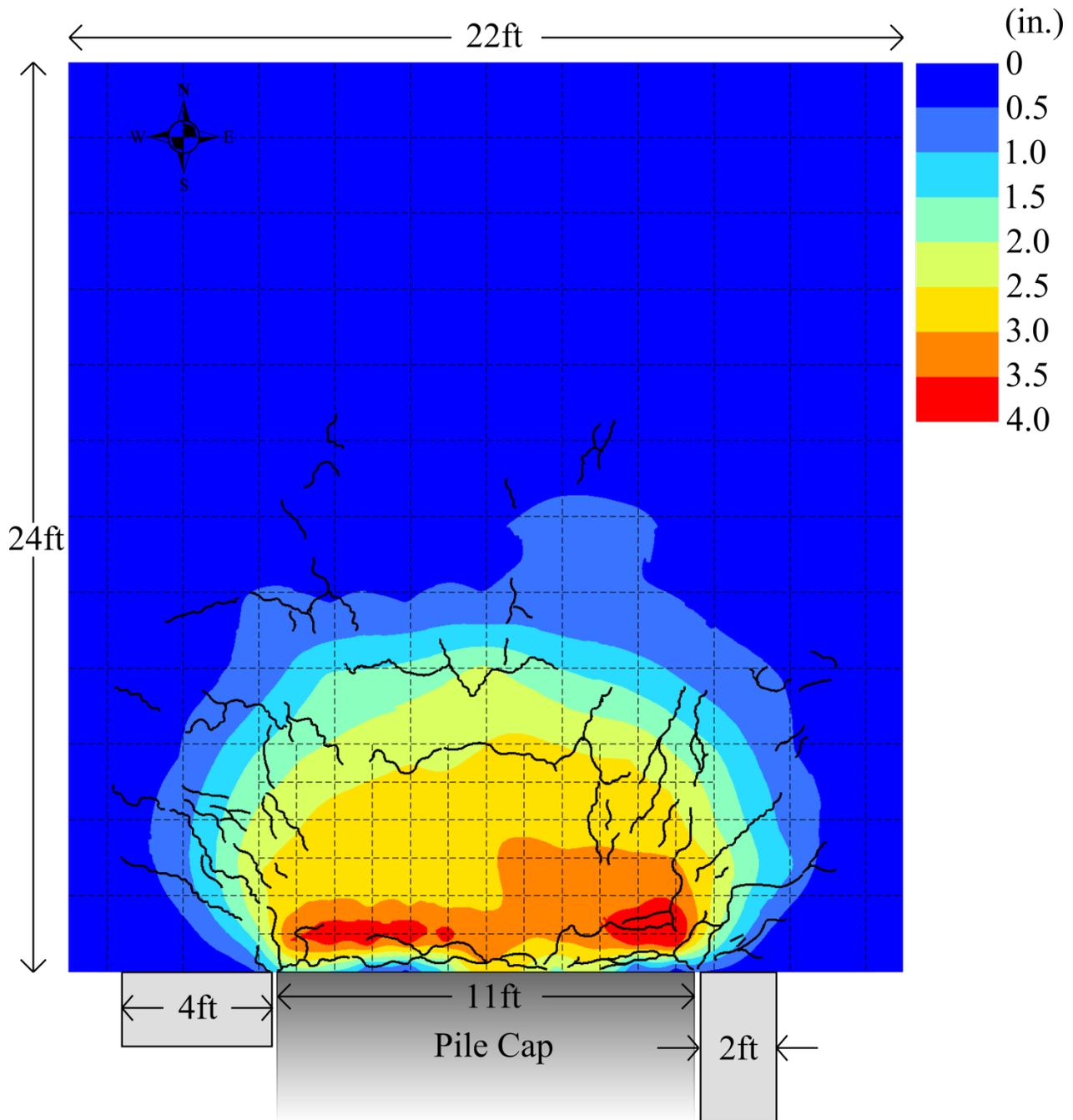
Figure 23. Heave contours (units in inches) and surface cracks at 3.0 in (7.61 cm) of longitudinal displacement (test completion) for 0° skew test (NOTE: 1 inch = 2.54 centimeters).

Because data from the 5.5 ft gravel backfill was used for the 30° skew passive force-deflection curve, heave contours are provided for the 5.5 ft backfill instead of the 3.5 ft backfill test. Much less heave occurred in the 5.5 ft backfill for the 30° skewed abutment compared to the 3.5 ft backfill for the

non-skewed abutment, likely due to the increased resistance of the increased backfill height. Maximum

heave of approximately 0.5 inch was observed near the acute side of the abutment 4 to 6 ft out from the

backwall.
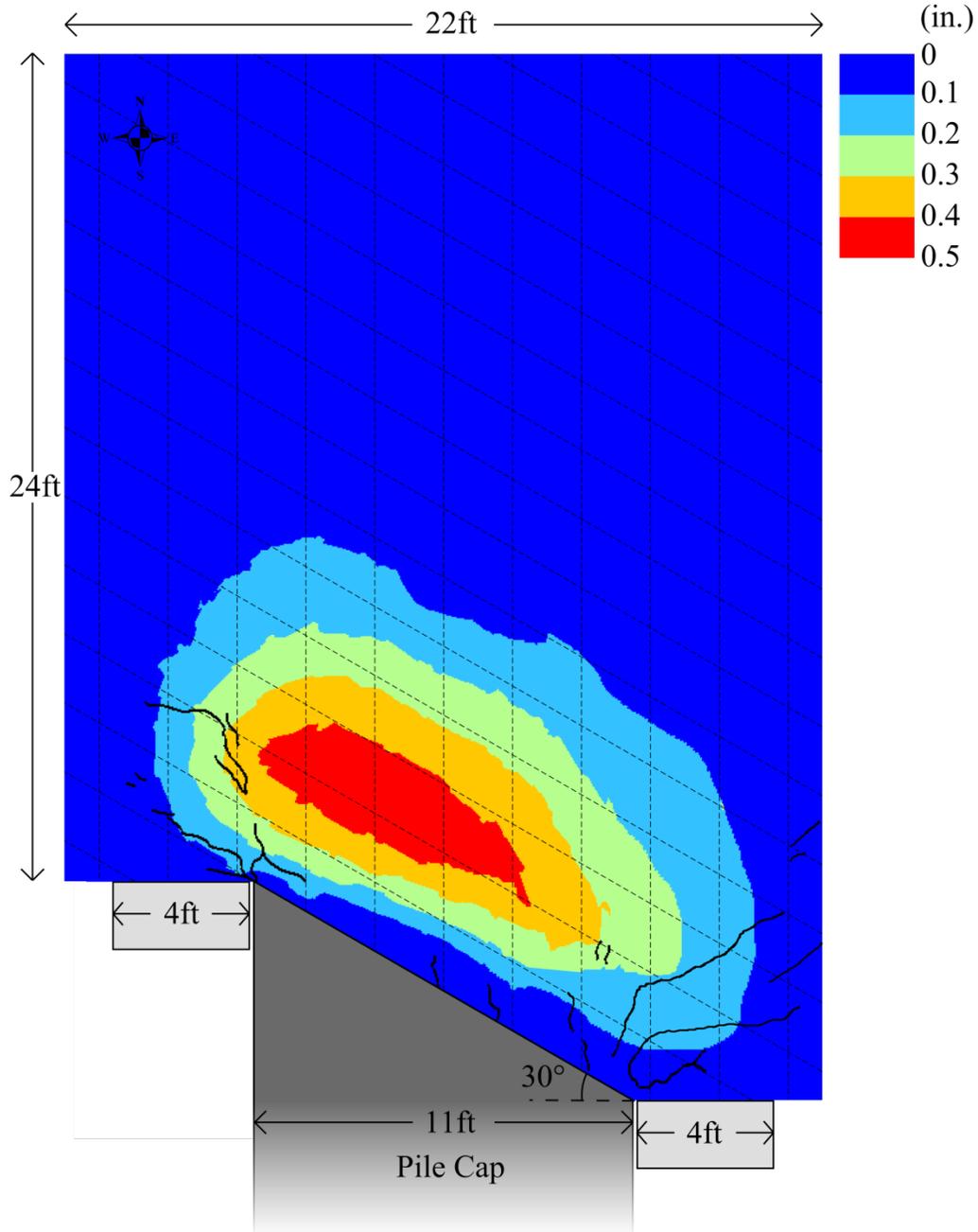
Figure 24. Heave contours (units in inches) and surface cracks at 2.5 in (7.61 cm) of longitudinal displacement (test completion) for 30° skew (NOTE 1 inch = 2.54 centimeters).

Horizontal backfill displacements for non-skewed and 30° skewed abutments are illustrated in Figure 25 and Figure 26. Displacement vectors for the non-skewed abutment typically indicate longitudinal movement of the backfill with an outward component near the edges of the wall. In contrast, the displacement vectors for the 30⁰ skew abutment typically show a significant transverse component in the direction of the acute side of the pile cap. This is particularly pronounced near the face of the wall and decreases somewhat with distance from the wall face.
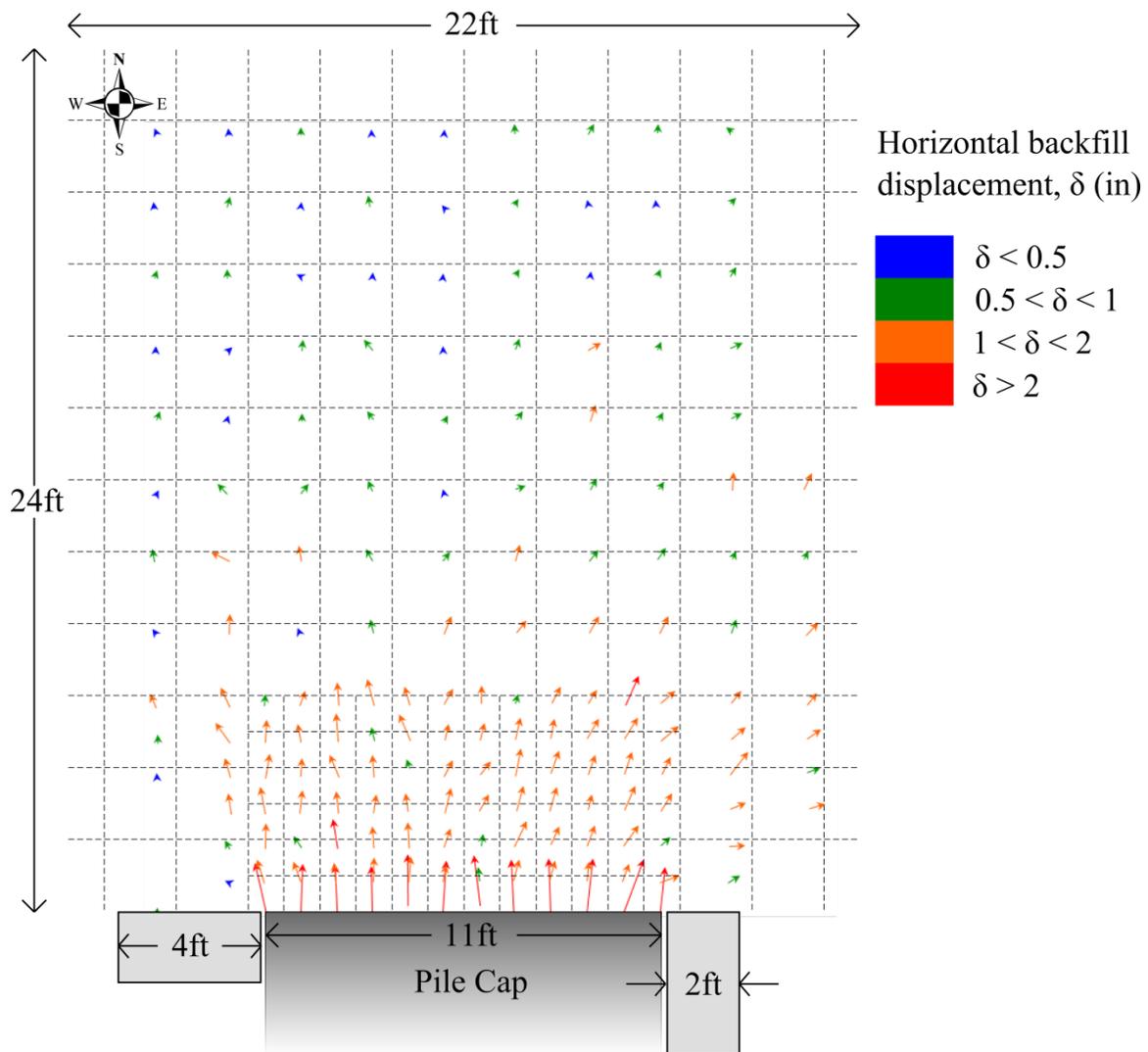
Figure 25. Soil displacement for 0° skew 3.5 ft. gravel backfill unconfined.
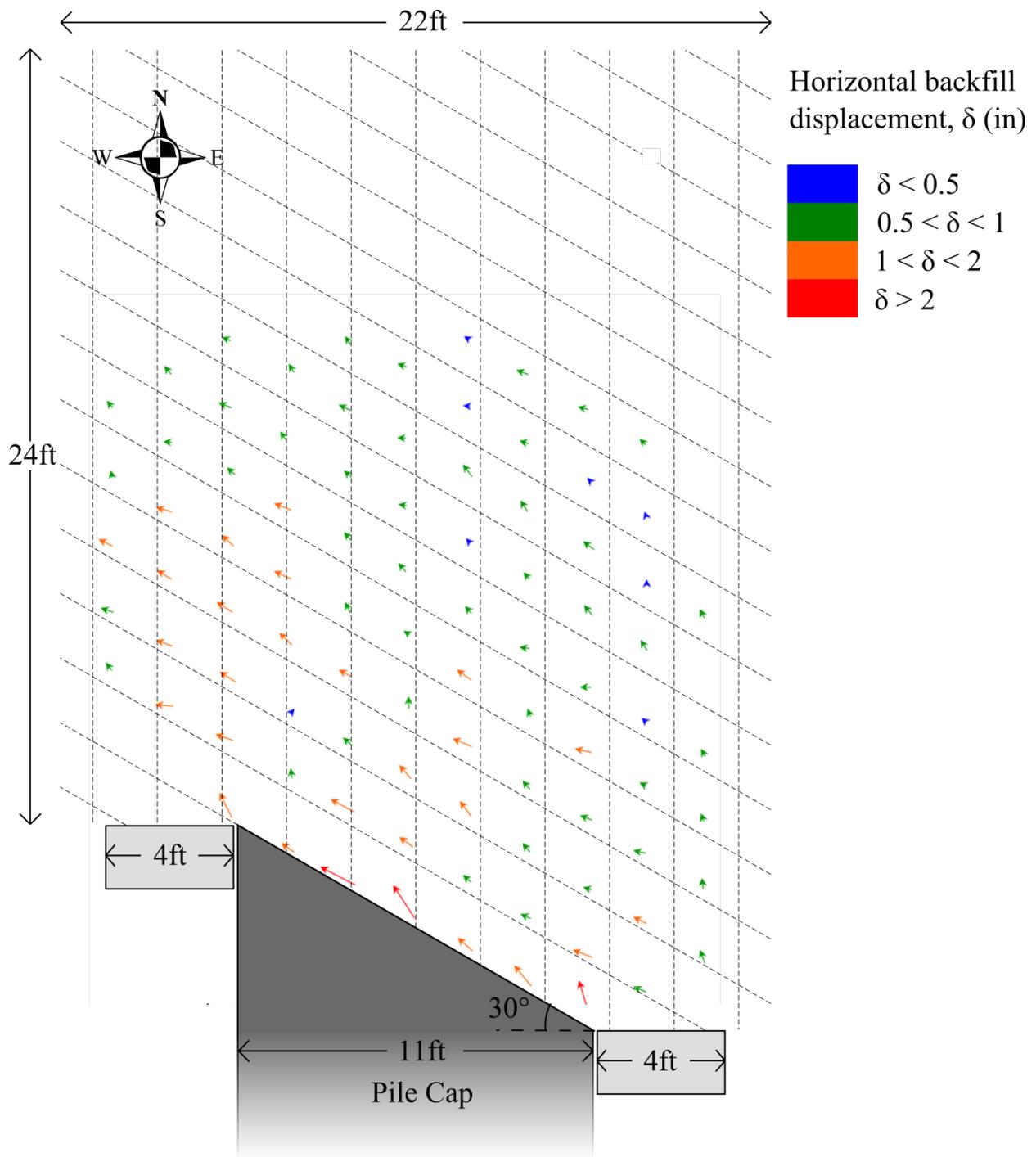
Figure 26. Soil displacement for 30° skew 5.5 ft. gravel backfill unconfined.

CONCLUSIONS

1. Field tests conducted in this investigation confirm results from lab tests and numerical analyses that there is a significant reduction in peak passive force as abutment skew angle increases.

2. Although these tests involved a dense sandy gravel backfill rather than clean sand backfill, the results obtained from the field test generally verify the reduction factor versus skew equation proposed by Rollins and Jessee (2013). However, the measured reduction factor is somewhat higher than the predicted value (0.58 vs 0.50) which may be a result of the higher friction angle of the backfill or simply natural variation in the test results. Additional tests would be necessary to investigate this issue further.

3. The general shape of heave and crack patterns were reasonably consistent with the previous tests on sand backfill. For the non-skewed case the patterns were symmetric about the centerline. However, for the skewed case, there was a concentration of heave towards the acute side of the pile cap and the cracks extended significantly beyond the acute side of the wall but were approximately normal to the obtuse side of the wall.

4. Displacement vectors were typically oriented longitudinally for the non-skewed case with some transverse component near the edges of the pile cap. In contrast, displacement vectors for the skewed case showed a significant transverse component in the backfill material which was most pronounced immediately adjacent to the pile cap.

ACKNOWLEDGMENTS

REFERENCES

AASHTO (2011). "Guide Specifications for LRFD Seismic Bridge Design." 3-106.

Apirakyorapinit, P., Mohammadi, J., and Shen, J. (2012). "Analytical Investigation of Potential Seismic Damage to a Skewed Bridge." *Practice Periodical on Structural Design and Construction*, 16(1), 5-12.

Burke Jr., M. P. (1994). "Semi-Integral Bridges: Movements and Forces." 1-7.

Caltrans (2001). "Seismic Design Criteria Version 1.2." California Department of Transportation, Sacramento, California.

Duncan, J. M., and Mokwa, R. L. (2001). "Passive Earth Pressures: Theories and Tests." *Journal of Geotechnical and Geoenvironmental Engineering, ASCE*, 127(3), 248-257.

Elnashai, A. S., Gencturk, B., Kwon, O., Al-Qadi, I. L., Hashash, Y., Roesler, J. R., Kim, S. J., Jeong, S., Dukes, J., and Valdivia, A. (2010). "The Maule (Chile) Earthquake of February 27, 2010: Consequence Assessment and Case Studies." Department of Civil and Environmental Engineering, University of Illinois at Urbana-Champaign, 190.

Lee, K. L., and Singh, A. (1971). "Relative Density and Relative Compaction." *Journal of Soil Mechanics and Foundations Design*, 97(7), 1049-1052.

Mokwa, R. L., and Duncan, J. M. (2001). "Experimental Evaluation of Lateral-Load Resistance of Pile Caps." *Journal of Geotechnical and Geoenvironmental Engineering, ASCE*, 127(2), 185-192.

Pruett, J. M. (2009). *Performance of a Full-Scale Foundation with Fine and Coarse Gravel Backfills Subjected to Static, Cyclic, and Dynamic*. M.S. Thesis, Brigham Young University, Provo, UT.

Rollins, K. M., and Cole, R. T. (2006). "Cyclic Lateral Load Behavior of a Pile Cap and Backfill." *Journal of Geotechnical and Geoenvironmental Engineering, ASCE*, 132(9), 1143-1153.

Rollins, K. M., Gerber, T., Cummins, C., and Herbst, M. (2009). "Monitoring Displacement vs. Depth in Lateral Pile Load Tests with Shape Accelerometer Arrays." *Proceedings of 17th International on Soil Mechanics & Geotechnical Engineering*, 3, 2016-2019.

Rollins, K. M., Gerber, T. M., Cummins, C. R., and Pruett, J. M. (2010). "Dynamic Pressure on Abutments and Pile Caps." *Report No. UT-10.18*, B. Y. University, U. D. o. Transportation, and F. H. Administration, eds., Utah Department of Transportation, 255.

Rollins, K. M., Gerber, T. M., and Heiner, L. (2010). "Passive Force-Deflection Behavior for Abutments with MSE Confined Approach Fills." *Report No. UT-10.15*, Utah Department of Transportation.

Rollins, K. M., and Jessee, S. (2012). "Passive Force-Deflection Curves for Skewed Abutments." *Journal of Bridge Engineering*, 17(5).

Rollins, K. M., and Sparks, A. E. (2002). "Lateral Load Capacity of a Full-Scale Fixed-Head Pile Group." *Journal of Geotechnical and Geoenvironmental Engineering, ASCE*, 128(9), 711-723.

Shamsabadi, A., Kapuskar, M., and Zand, A. (2006). "Three-Dimensional Nonlinear Finite-Element Soil-Abutment Structure Interaction Model for Skewed Bridges." *5th National Seismic Conference On Bridges and Highways*, FHWA, ed.San Francisco, CA, 1-10.

Shamsabadi, A., Rollins, K. M., and Kapaskur, M. (2007). "Nonlinear Soil-Abutment-Bridge Structure Interaction for Seismic Performance-Based Design." *Journal of Geotechnical and Geoenvironmental Engineering, ASCE*, 133(6), 707-720.

Steinberg, E., and Sargand, S. (2010). "Forces in Wingwalls from Thermal Expansion of Skewed Semi-Integral Bridges." *Report No. FHWA/OH-2010/16*, Prepared by Ohio University for Ohio Department of Transportation, Athens, OH, 87.

Strassburg, A. N. (2010). "Influence of Relative Compaction on Passive Resistance of Abutments with Mechanical Stabilized Earth (MSE) Wingwalls."M.S. Thesis, Brigham Young University, Provo, UT.

Unjohn, S. "Repair and Retrofit of Bridges Damaged by the 2010 Chile, Maule Earthquake." *Proc., International Symposium on Engineering Lessons Learned from the 2011 Great East Japan Earthquake*.